Applications of SANS to Study Membrane Protein Systems

12

Frank Gabel

Abstract

Small angle neutron scattering (SANS) is a powerful tool to obtain structural information on solubilized membrane proteins on the nanometer length-scale in complement to other structural biology techniques such as cryo-EM, NMR and SAXS. In combination with deuteration of components and/or contrast variation (H_2O:D_2O exchange in the buffer) SANS allows to separate structural information from the protein and the detergent/lipid parts in solution. After a short historical overview on results obtained by SANS on membrane protein systems, this book chapter introduces the basic theoretical principles of the technique as well as requirements on samples. The two introductory sections are followed by an illustration of the specific consequences of sample heterogeneity of solubilized membrane proteins in the presence of detergent/lipid molecules on the interpretation of structural information by using simple, geometric models. The next sections deal with more sophisticated modelling approaches including *ab initio* shape reconstructions and full-atomic models in the presence of detergent/lipid and specific results obtained by these approaches. After a short comparison with the SAXS technique, this book chapter concludes with an overview of present and

F. Gabel (✉)
Université Grenoble Alpes, Institut de Biologie Structurale, 38044 Grenoble Cedex 9, France

Commisariat à l'Energie Atomique et aux Energies Alternatives, Direction de la Recherche Fondamentale, Institut de Biologie Structurale, 38044 Grenoble Cedex 9, France

Centre National de la Recherche Scientifique, Institut de Biologie Structurale, 38044 Grenoble Cedex 9, France

Large Scale Structures Group, Institut Laue-Langevin, 38042 Grenoble Cedex 9, France
e-mail: frank.gabel@ibs.fr

B. Chaudhuri et al. (eds.), *Biological Small Angle Scattering: Techniques, Strategies and Tips*, Advances in Experimental Medicine and Biology 1009, DOI 10.1007/978-981-10-6038-0_12

future developments and impact that can be expected by SANS on membrane structural biology in the coming years.

Keywords
Contrast variation • Heavy water • D_2O • Deuteration • Form factor • MD simulation • Shape • Low resolution • Detergent • Lipid • Protein

12.1 Historical Overview

The application of small-angle neutron scattering (SANS) for the structural study of (weakly scattering) biological systems such as solubilized membrane proteins became technically feasible with the advent of high-flux neutron sources in the 1960s and 1970s. Earliest work, carried out at the Institut Laue-Langevin (Grenoble, France) and at the High Flux Beam Reactor (Brookhaven, USA) includes studies on several membrane protein systems purified directly from biological tissues: human serum low-density lipoprotein (Stuhrmann et al. 1975), bovine and frog rhodopsin (Osborne et al. 1978; Yeager 1976), the acetylcholine receptor from *Torpedo californica* (Wise et al. 1979) and porcine pancreatic colipase (Charles et al. 1980). Most of this early work was able to provide important model-free parameters of the protein-detergent complexes such as radii of gyration R_G of both the complex and the individual partners, their stoichiometry, and molecular masses. The qualitative relative arrangements (in particular the distances) between protein and detergent moieties were obtained by a Stuhrmann analysis (Stuhrmann 1973), i.e. by interpreting the change of the measured R_G at different contrast conditions (H_2O:D_2O ratio in the solvent), occasionally combined with deuterated detergent to enhance contrast. In some cases, simple geometrical bodies were proposed for the protein and detergent moieties (Wise et al. 1979; Charles et al. 1980). Even though the functional interpretations of these pioneering results were limited in the absence of atomic-resolution structures, they allowed to probe and validate (or discard) basic working models of the membrane proteins studied. A more exhaustive overview on early SANS results from membrane protein systems can be found elsewhere (Timmins and Zaccai 1988).

In the second half of the 1980s the routine use of recombinant protein expression (Atkinson and Small 1986) made a wider range of membrane protein systems accessible to SANS, in particular in combination with an increasing commercial availability of deuterated detergent molecules. Concomitantly, more sophisticated modelling approaches using a number of beads to represent protein shapes were being developed (Perkins and Weiss 1983). The investigation of atomic-resolution membrane protein models became available in the 1990s with the first structures being deposited in the protein data bank (PDB) and the development of computer programs to back-calculate SANS curves efficiently from them (Svergun et al. 1998). At the same time, *ab initio* shape analysis was being developed (Svergun 1999; Chacon et al. 1998) and since the turn of the millennium, an increasingly versatile toolbox of computer programs for the interpretation of SANS data, including rigid body modeling and the comparison to cryo-EM data has become available (Zaccai et al. 2016; Chaudhuri 2015; Petoukhov et al. 2012). In parallel, ever more sophisticated labeling schemes (e.g. partial deuteration) became available for detergent/lipid molecules (Hiruma-Shimizu et al. 2016; Haertlein et al. 2016; Maric et al. 2015) to fine-tune contrast matching approaches.

12.2 Neutron Scattering Theory and Experimental Considerations

The general theory of small-angle scattering (SAS) as well as the specific theory and experimental setup for general SANS experiment have been introduced in previous sections of this book or in recent reviews and I will summarize here only briefly specific points related to membrane protein systems (Clifton et al. 2013).

The SANS signal measured from a solution of arbitrarily oriented particles i (after solvent subtraction) corresponds to a one-dimensional intensity I versus the modulus of the wave vector $\boldsymbol{q}$ and can be expressed as follows:

$$I(q) = \sum_i N_i \left\langle \left| \int \Delta\rho_i e^{i\vec{q}\cdot\vec{r}} dV_i \right|^2 \right\rangle, \quad q = \frac{4\pi}{\lambda}\sin\theta \tag{12.1}$$

Where λ is the neutron wavelength and 2θ the scattering angle. N_i is the number of particles of a distinct species i. For solubilized membrane proteins these species correspond in practice to protein-detergent/lipid complexes (PDC), protein-free detergent/lipid aggregates (such as micelles, vesicles etc.) and single, free detergent and/or lipid molecules (Fig. 12.1). $\Delta\rho_i$ is the neutron scattering length density (SLD) contrast of specific particles with respect to the solvent. It varies in general for neutrons between protein and detergent/lipid head- and tail-groups (Timmins and Zaccai 1988; Jacrot 1976) (Fig. 12.2) and therefore has to be integrated over the whole particle volume V_i. The broken brackets correspond to a rotational average over all possible particle orientations.

Figure 12.2 represents the basics of contrast variation, that is the possibility by SANS to minimize the signal of either detergents/lipids or

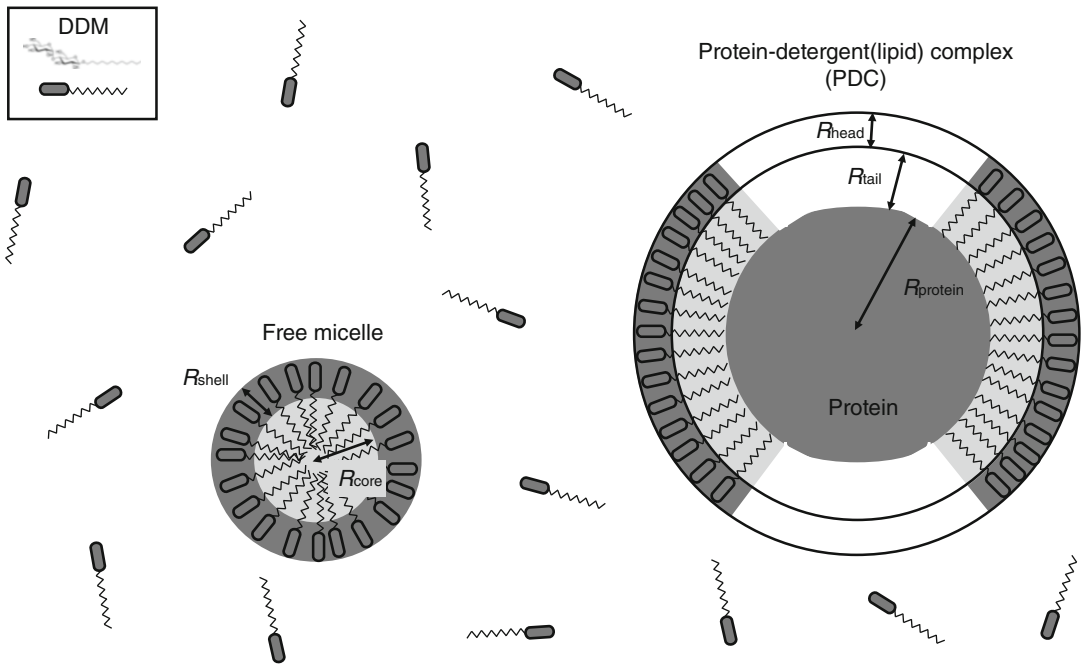

Fig. 12.1 Schematic representation of compounds in a solubilized membrane protein sample. This schematic and strongly simplified overview shows a selection of individual particles in a sample of DDM (n-Dodecyl β-D-maltoside)-solubilized membrane proteins: free detergent molecules, free micelles, and the protein-detergent/lipid complex (PDC). The designations of geometric parameters (radii, thicknesses) in this figure correspond to the ones used in the following sections. *Different shades of grey* symbolize different contrasts $\Delta\rho$ (Table 12.1)

protein by measuring at an appropriate H_2O:D_2O ratio and to focus on structural information from specific parts of a complex membrane protein system. Reasonable signal/noise on the most performant present-day SANS instruments can be obtained from membrane protein solutions in the (protein) concentration range 1–10 mg/mL for protein molecular masses in the range from ~20 kDa to several 100 kDa and for 100–200 μL sample volumes with exposure times varying between a few minutes and several hours, depending on contrast and instrumental setup.

As in the case of water-soluble proteins, mastery of the biochemistry and sample preparation prior to the experiment is of paramount importance for the interpretation of the experimental SANS curves in terms of structural parameters (Jacques and Trewhella 2010). For solubilized membrane proteins in particular, the monodispersity of the PDC and the detergent/lipid aggregates should be checked by preliminary complementary techniques including analytical ultracentrifugation (AUC) and size-exclusion chromatography (SEC) (Le Roy et al. 2015; le Maire et al. 2000). Ideally, the buffer subtracted from the sample containing the protein should match the latter in concentration of individual detergent/lipid molecules as well as free detergent/lipid aggregates (e.g. micelles) in order to eliminate their contribution to the SANS signal completely. If feasible, the buffer from the last purification (gel filtration) step should be used without further concentration if the detergent/lipid aggregate sizes and shapes depend on concentration.

Three major criteria should be respected when considering the choice of a detergent/lipid system for solubilizing membrane proteins for SANS experiments: (1) the detergent/lipid system should solubilize the membrane protein in a stable, monodisperse complex and in a functionally relevant state, (2) the contrast between protein and detergent/lipid (Fig. 12.2) should be chosen as high as possible and (3) protein-free detergent/lipid aggregates should be kept at a minimal concentration and as monodisperse as possible, i.e. in practice large aggregates such as vesicles, rod-like structures etc. should be avoided in order not to dominate the protein signal (see also following section). Point (3) requires a good knowledge of the detergent/lipid phase diagram and in particular the critical micellar concentration (CMC) (le Maire et al. 2000; Helenius and Simons 1975).

12.3 Influence of Membrane Protein Sample Heterogeneity on the SANS Signal: A Simple Geometrical Case Study

The extraction and interpretation of structural information by small angle neutron scattering according to Eq. 12.1 requires that the membrane proteins be solubilized in the presence of detergent and/or lipids. The required experimental conditions give rise to a composite system of (at least) three chemically different components with specific and distinct scattering length densities (SLDs): protein, detergent/lipids and (aqueous) solvent. In many cases, several distinct particulate species are formed (we exclude non-particulate systems such as lamellar phases, interconnected networks etc. (Qian and Heller 2015; Harroun et al. 2005; Seddon et al. 2004) and their respective scattering contributions need to be described separately: free (single) detergent/lipid molecules, protein-free detergent/lipid aggregates (micelles, vesicles etc.) and protein-detergent/lipid complexes (PDC) (Fig. 12.1). The general equation of the measured intensity (Eq. 12.1) can thus be rewritten as follows:

$$
\begin{aligned}
&I(q) \\
&\propto N_{PDC}\,\langle |M_{prot}A_{prot}(q) + M_{lipid\_bound}\,A_{lipid\_bound}\,(q)|^2\rangle \\
&\quad + N_{aggregates}\,\langle |M_{lipid\_aggregates}\,A_{lipid\_aggregates}\,(q)|^2\rangle \\
&+N_{free}\,\langle |M_{lipid\_free}\,A_{lipid\_free}\,(q)|^2\rangle
\end{aligned}
\tag{12.2}
$$

N_{PDC}, $N_{aggregates}$ and N_{free} designate the number of particles of the respective species in solution. A_{prot}, A_{lipid_bound}, $A_{lipid\_aggregates}$ and A_{lipid_free} correspond, respectively, to the scattering amplitudes (form factors) of the protein, the lipids/detergents bound to it, the lipids/detergents

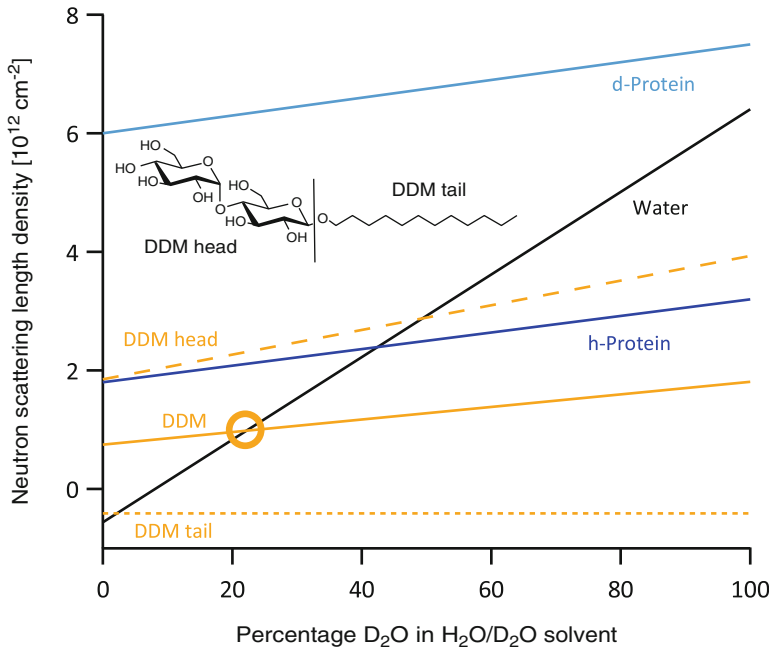

Fig. 12.2 Neutron scattering length densities (SLD) ρ of proteins and DDM detergent. The values are calculated from literature (Jacrot 1976; Breyton et al. 2013a). The contrast $\Delta\rho$ (Eq. 12.1) at a given H_2O:D_2O ratio of each compound/moiety is defined as the difference between its own SLD and the one of the solvent (mixture of ordinary and heavy water). The *orange circle* indicates the contrast match point (CMP, i.e. $\Delta\rho = 0$) of an entire DDM molecule (head- plus tail-group) at ~22% D_2O. h-protein is a natural, hydrogenated protein, d-protein is a perdeuterated protein (all hydrogens replaced by deuterium). In general, all hydrogenated proteins have similar SLDs as the one depicted here while the SLDs for different detergents can deviate significantly from those of DDM (Breyton et al. 2013a)

associated in protein-free aggregates (micelles, vesicles etc.) and the free, single lipid/detergent molecules (for the sake of simplicity we use the index "lipid" in Eq. 12.2 for both lipid and detergent molecules). M_i are the scattering masses of the respective parts of the systems and are given by $\int \Delta\rho_i \, dV_i$.

The significance and impact of Eq. 12.2 on the interpretation of SANS data is illustrated by a simplified model system consisting of a (hypothetical) spherical membrane protein covered entirely by a monolayer of detergent in addition to free, spherical micelles (Fig. 12.1). For the explicit calculations (see details in the Appendix), we assumed a hydrogenated protein and DDM (n-Dodecyl-β-D-maltopyranoside) detergent molecules at both 0 and 22% D_2O, the latter contrast corresponding to the overall contrast match point (CMP) of DDM detergent molecules (Fig. 12.2). The contrasts of the individual components are listed in Table 12.1 and in all cases random orientations of all individual components are assumed.

At 0% D_2O (DDM not matched) the presence of bound detergent modifies both the intensity and the form factor of the protein (Fig. 12.3a, blue line vs continuous red line) and increases its apparent size (increase of $I(q = 0)$ intensity by a factor of 2.5 and radius of gyration R_G by 24% from 31.4 to 38.8 Å). The relative contribution to the signal of free micelles (green line) with respect to the PDC complex (red line) is about 8% in intensity (at a stoichiometry 10:1) at small angles and reduces the R_G of the PDC by 3% (to 37.7 Å). More importantly, their presence modifies the scattering curve from the complex

significantly at intermediate q-ranges (0.07...0.25 Å^{-1}) (red continuous vs broken lines). Therefore, SANS curves of PDC complexes (in the absence or presence of additional free micelles) for non-matched detergent/lipids cannot, in general, be interpreted in terms of molecular mass or shape of the embedded proteins alone.

At 22% D_2O (CMP of DDM), free micelles scatter very weakly at low angles ($q < 0.05$ Å^{-1}) with respect to the solubilized proteins and their contribution to $I(0)$ and the R_G can be neglected, even in tenfold molar excess with respect to the PDC complexes (Fig. 12.3b, green and red broken lines). At intermediate q-values (0.07...0.25 Å^{-1}) the situation is similar to the one at 0% D_2O with a modification of the signal from the isolated PDC complex (red lines). The situation is more complex for protein-bound detergent: even though matched on average at 22% D_2O and therefore not modifying the $I(0)$ intensity and the apparent molecular mass of the protein, the form factor of the PDC complex is not the same as the one of the isolated protein alone (blue vs continuous red line) but increases the R_G by 14% from 31.4 to 35.7 Å. This effect is due to the specific spatial arrangement and contrast of detergent moieties with respect to the protein: tail-groups are closer to the protein and have negative contrast while head-groups are further away from the protein and have positive contrast (Table 12.1). While their respective contributions to the scattered intensity (Eq. 12.1) cancels in the forward scattering direction $I(q = 0)$, they do not annihilate for $q > 0$.

While instructive regarding the sensitivity of SANS signal from complex, solubilized membrane protein systems regarding internal SLD heterogeneity and sizes of different particles, the analytical analysis presented here is heavily oversimplified with respect to several aspects: assumption of a spherical protein, covered homogeneously and completely by a double layer representing a head- and tail-group of detergent/lipid molecules, and a monodisperse and spherical population of micelles, composed of neatly separated homogeneous layers. More accurate descriptions of realistic systems would include non-spherical proteins, covered only partly by detergent/lipids and ellipsoidal micellar structures (Lipfert et al. 2007) as well as polydispersity in micellar size (Manet et al. 2011). These modifications would qualitatively lead to more smeared minima of the idealized calculated curves here but would not change the overall conclusions. Unfortunately, form factors of geometrical bodies that deviate even slightly from the spherical shape (e.g. ellipsoids, cylinders etc.) can no longer be written explicitly but are represented by mathematical integrals that need to be solved numerically (Pedersen 2002). Finally, it should be noted that the conclusions drawn here on micellar detergent/lipid aggregates as "contaminants" of the SANS signal of solubilized membrane proteins are even more pronounced when larger aggregates such as vesicles, liposomes or rods are present (Rubinson

Table 12.1 SLD differences (i.e. contrast) $\Delta\rho$ of individual components shown in Figs. 12.1, 12.2, and 12.3

$\Delta\rho$component (10^{10} cm^{-2})	**0% D_2O**	**22% D_2O**		
Protein	2.36	1.12		
DDM head	2.41	1.34		
DDM tail	0.15	−2.51		
Radii and thicknesses (Å)	**Protein**	**DDM head**	**DDM tail**	**Whole particle**
Free DDM molecule	*	*	*	*
Free DDM micelle	*	5.3	20	25.3
Free protein	40	*	*	40
Protein-detergent complex (PDC)	40	4.8	6	50.8

The geometrical components were chosen to approach published values on DDM molecules (Oliver et al. 2013) but also to yield a matched intensity ($I(0) = 0$) at 22% D_2O

* *ND*

et al. 2013; Qian and Heller 2011; Breyton et al. 2009; Hunt et al. 1997).

12.4 Strategies to Minimize/Homogenize the Detergent/Lipid SANS Signal and Shape Analysis

The previous section illustrates that the internal (SLD) heterogeneity of detergent/lipid molecules and their presence both in the protein-detergent/lipid complex and in the form of free micelles has a strong impact on the interpretation of membrane protein structures by SANS experiments. While it is in general reliable to extract molecular masses of membrane proteins from the $I(0)$ intensity at the detergent/lipid contrast match point (Fig. 12.3b, $I(0)$ intensities of blue and red curves) and therefore determine their oligomeric state (Compton et al. 2011), other elementary structural parameters such as the radius of gyration (R_G) cannot be interpreted as due to the protein alone. Moreover, *ab initio* shape analysis using single phases such as DAMMIN (Svergun 1999) will yield erroneous envelopes, encompassing both bound detergent/lipid molecules as well as a weighted contributions of micellar features from intermediate q-ranges (Fig. 12.3, deviations between red broken lines from red continuous lines). Several strategies have therefore been applied in literature to focus on the signal of the embedded membrane protein and to minimize the signal due to protein-bound detergent/lipid and/or free detergent/lipid aggregates:

1. **Reinforcing contrast by deuteration**: the relative contribution of internal SLD fluctuations of free detergent/lipid aggregates can be minimized by either increasing the signal of the protein by its deuteration in the presence of hydrogenated detergents/lipids or by working with deuterated lipids/detergents and hydrogenated proteins at elevated D_2O percentages in the solvent (Compton et al. 2011; Gabel et al. 2014). In the former approach, the contrast of the deuterated protein (d-protein, Fig. 12.2) is much larger than the SLD fluctuations between head/tail of the detergent/lipid molecules which can be neglected in favorable cases, in particular for small differences between head/tail SLDs (Breyton et al. 2013a), by choosing detergent/lipids with low aggregation numbers close to their CMC (le Maire et al. 2000) or when only a few detergent/lipid molecules are attached to a protein complex of very large size (Efremov et al. 2015). Deuteration of lipids has the advantage of homogenizing the internal SLD variation for certain detergents/lipids (Timmins and Zaccai 1988; Breyton et al. 2013a) and, in addition, allows to work at high D_2O concentrations which minimizes incoherent neutron scattering background (Gabel et al. 2002) and therefore improves signal/noise.
2. **Homogenizing internal contrast of detergents/lipids**: while internal SLD fluctuations between head- and tail-groups of detergent/lipid molecules can often be reduced by deuteration (see above), full deuteration unfortunately leads to SLD that can no longer be matched, even when working in 100% D_2O (Breyton et al. 2013a). Alternatively, some detergent molecules have small SLD fluctuations in their natural (hydrogenated) state, e.g. fluorinated surfactants (Breyton et al. 2013b). Some of these compounds, however, have a match point close to 40% D_2O and therefore require the use of deuterated proteins for structural studies by SANS. Another strategy consists in mixing hydrogenated and deuterated detergents/lipids at appropriate ratios in order to obtain a desired match point (Osborne et al. 1978; Clifton et al. 2012). Finally, more complex systems such as nanodiscs (mixed polypeptide/detergent/lipid particles) have been used recently to solubilize membrane proteins (Kynde et al. 2014; Skar-Gislinge et al. 2010; Bayburt and Sligar 2010; Nakano et al. 2009). In some cases (so-called "stealth nanodiscs"), the systems were designed to be matched out relatively homogeneously at

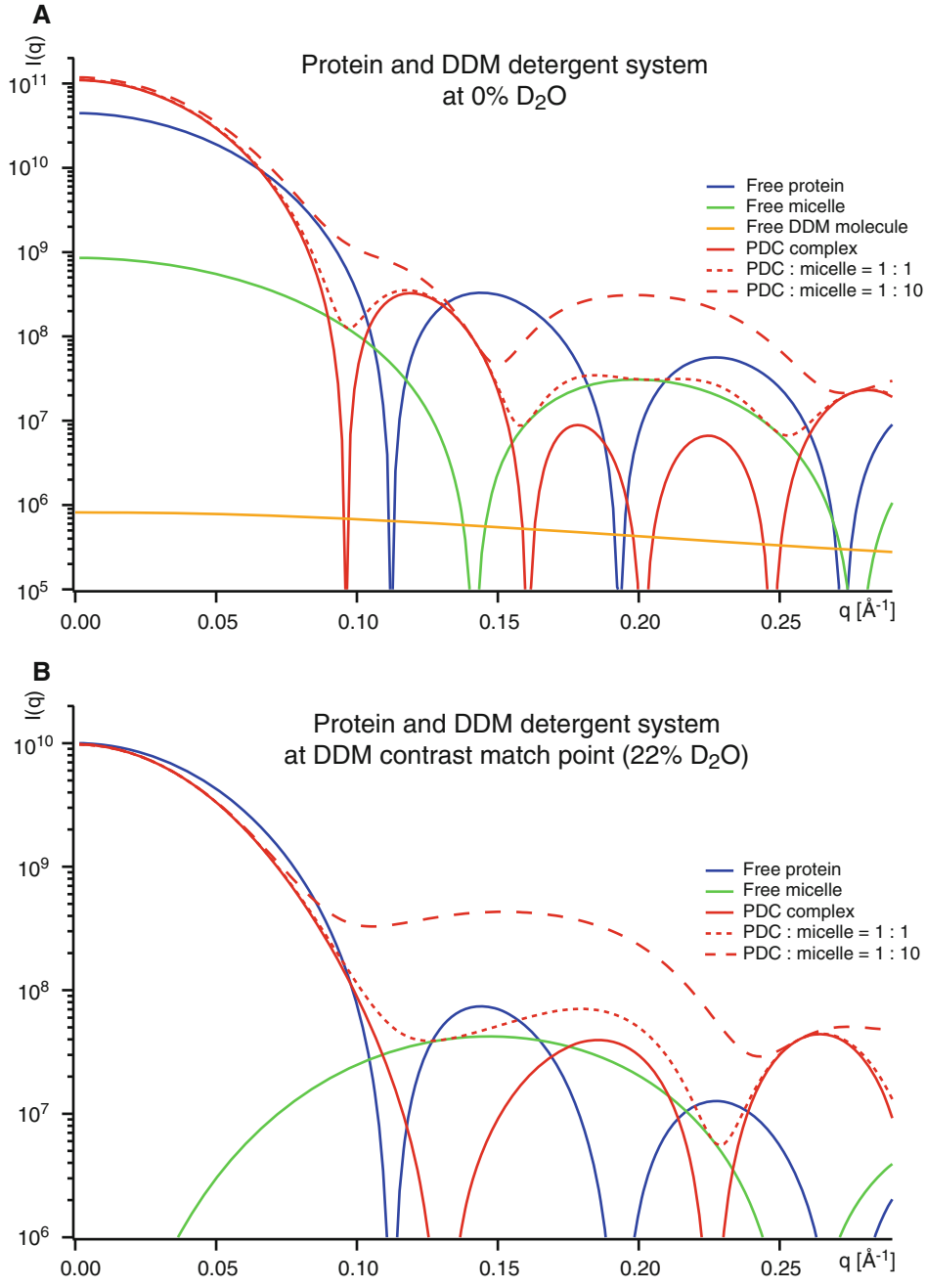

Fig. 12.3 Theoretical SANS curves of simple, composite membrane protein systems at 0% (**a**) and 22% (**b**) D_2O. SANS curves calculated for free protein, free DDM micelle, isolated PDC complex and mixtures of PDC and micelles at two different stoichiometric ratios. The curves were calculated with Eq. 12.2 and the equations presented in the Appendix, by using neutron scattering length densities from literature (Jacrot 1976; Breyton et al. 2013a), listed in Table 12.1, and represent faithfully the relative intensities. The geometrical shapes of the micelle and PDC were assumed to be spherical as in Fig. 12.1, with the additional assumption that a detergent monolayer covers the protein completely (*black lines*, Fig. 12.1). The numerical values of the different parameters (protein radius, micelle core and shell radii and detergent head and tail lengths) are detailed in Table 12.1. The SANS curve of an individual DDM molecule was calculated with CRYSON (Svergun et al. 1998) using its atomic structure from the PDB (ligand ID entry "LMT")

about 100% D_2O allowing thus the study of hydrogenated membrane proteins with very good signal/noise (Maric et al. 2014).

The strategies (1) and (2) allow, in a more or less accurate way, to assume that the detergents/lipids can be considered to be homogeneous (in terms of SLD fluctuations between head- and tail-groups) and that the measured SANS signal at their contrast match point is due exclusively to the solubilized membrane proteins themselves. Under these conditions, the same approaches developed for water-soluble proteins have been applied on membrane proteins, in particular single- (Compton et al. 2011, 2014; Breyton et al. 2013b; Le et al. 2014; Sharma et al. 2012; Tang et al. 2010; Nogales et al. 2010; Cardoso et al. 2009; Zimmer et al. 2006; Johs et al. 2006; Bu et al. 2003) and multi-phase (Clifton et al. 2012) *ab initio* shape reconstructions. In the latter case, both detergents/lipids and protein are represented by two distinct envelopes and it is possible to determine their relative shapes and positions simultaneously by fitting SANS curves at multiple contrasts, e.g. with the program MONSA (Svergun 1999; Petoukhov and Svergun 2006).

12.5 Full-Atomic and Other Sophisticated Modelling Approaches

The previous section assumes that deuteration strategies allow to interpret SANS signals from complex systems (PDC plus free detergent/lipid aggregates) exclusively in terms of the protein structure at the detergent/lipid contrast match point. This is unfortunately not possible in all experimental cases and in general, a non-negligible contribution of bound detergent/lipid as well as free detergent/lipid aggregates to the overall SANS signal needs to be taken into account. Size exclusion chromatography, coupled to SANS (SEC-SANS), which in analogy to SEC-SAXS experiments would allow the separation of the PDC from detergent/lipid aggregates such as micelles (see next section), has been developed recently (Jordan et al. 2016) but has not been applied, to our best knowledge, to membrane protein systems so far.

An accurate approach if SANS signals of detergent/lipid molecules cannot be neglected due to internal heterogeneity or due to perdeuteration, is to model the PDC with several distinct parts, including detergent/lipid molecules. Several studies have applied coarse-grain/dummy-atoms or simple geometric models of detergent/lipids (Kynde et al. 2014; Tang et al. 2010; Cardoso et al. 2009; Gohon et al. 2008) to represent the internal heterogeneity, including between different detergent/lipid moieties such as head- and tail groups. In some cases, full-atom detergent/lipid models have been produced by MD simulations (Gabel et al. 2014; Le et al. 2014). When integrating SANS datasets from different contrasts, these sophisticated approaches allow to distinguish between modestly different protein conformations as well as to fine-tune the shape and topology of the bound detergent/lipid molecules (Fig. 12.4). The combination of MD simulations with SANS (and SAXS) data from membrane protein systems is a very active field at the moment and diverse new approaches are being developed (Perez and Koutsioubas 2015; Chen and Hub 2015). Importantly, care needs to be taken that the programs that back-calculate SANS curves from membrane protein complexes take exchangeable hydrogens from detergent/lipid molecules correctly into account.

12.6 Comparison with Small-Angle X-Ray Scattering (SAXS)

The SANS sister technique, small-angle X-ray scattering (SAXS) has been used for several decades to characterize solubilized detergents (Bouwstra et al. 1993) and has provided models for the shapes and internal structure of isolated micelles (Oliver et al. 2013; Lipfert et al. 2007; D'Andrea et al. 2011; Gobl et al. 2010) and nanodiscs (Skar-Gislinge and Arleth 2011). SAXS has also been used as a high-throughput

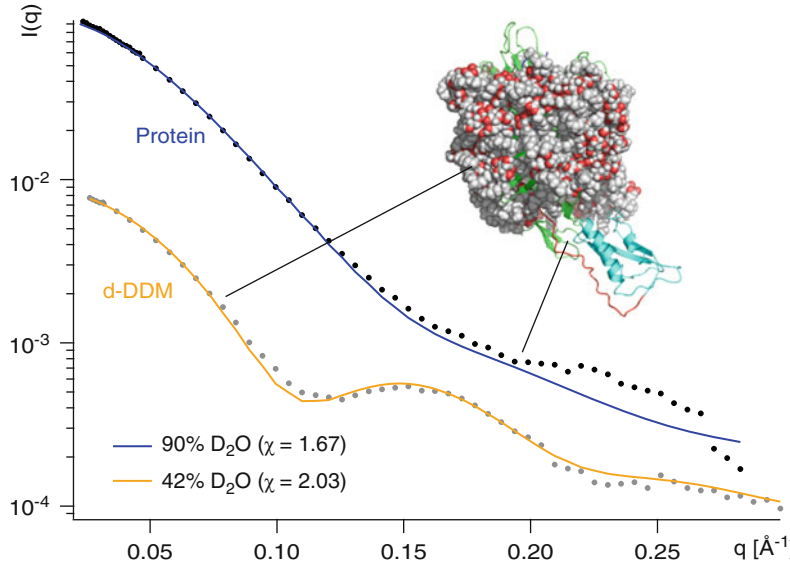

Fig. 12.4 Full-atomic model of membrane protein FhaC, including deuterated d-DDM detergent. The structural model displayed was fitted against SANS data in solution at 42 and 90% D_2O (contrast match points of protein and d-DDM, respectively) using the program CRYSON (Svergun et al. 1998). Detergent was built by MD simulations. Both SANS data sets were recorded at the instrument D22 at the Institut Laue-Langevin (ILL Grenoble, France) during 20 min at a protein concentration of 13 mg/mL. The figure was created based on data published by Gabel et al. (2014)

tool to probe crystallization phases (Joseph et al. 2011). First applications of SAXS to model solubilized membrane proteins in the presence of lipids/detergent are more recent (O'Neill et al. 2007; Columbus et al. 2006; Watanabe and Inoko 2005; Hong et al. 2004; Haas et al. 2004). While it was possible in some favorable cases to describe protein-detergent complexes by *ab initio* models using "static" SAXS experiments (Calcutta et al. 2012) the strong scattering contribution from detergent aggregates such as free micelles represents in general an important obstacle to such approaches. Due to their elevated electronic density, most detergent and lipid molecules cannot be easily contrast matched by the solvent and SAXS is therefore limited to a small number of compounds (Lipfert et al. 2007; Bu and Engelman 1999). A major breakthrough in recent years has been the advent of online size-exclusion chromatography (SEC), coupled to SAXS, which allowed to separate protein-detergent complexes from micelles and to apply sophisticated modeling approaches (Perez and Koutsioubas 2015; Dovling Kaspersen et al. 2014; Koutsioubas et al. 2013; Berthaud et al. 2012; Wright et al. 2011). Another promising recent development, so far specific to SAXS, are microfluidic platforms (Kondrashkina et al. 2013; Khvostichenko et al. 2013) that would allow the application of kinetic experiments to membrane protein systems.

12.7 Conclusions and Outlook

The past 10 years have witnessed an increasing number of SANS applications on solubilized membrane systems, as well as a rising level of sophisticated data interpretation (multiphase and full-atomic modelling) and biochemical sample preparation (deuteration strategies and choice of detergent/lipid/nanodisc systems). The ensemble of studies presented here illustrates that SANS is gaining momentum as a complementary structural biology technique to crystallography, cryo-EM and NMR and continues to provide

valuable new insights into membrane protein function. Recently, SANS has also been used as a tool to optimize and tune detergent/lipid arrangements to solubilize and to study membrane proteins (Ashkar et al. 2015; O'Malley et al. 2011). It can be expected that over the next 5–10 years exciting new developments in instrumentation, sample environment, biochemistry and data analysis will help to improve the accuracy of SANS data from membrane proteins and the structural questions that can be addressed. Some recent developments that will gain momentum include SEC-SANS, MD simulations (Le et al. 2014; Chen and Hub 2015; Herrera et al. 2014; Perlmutter et al. 2011) and new labeling schemes for detergent/lipid compounds (Hiruma-Shimizu et al. 2016; Haertlein et al. 2016; Maric et al. 2015; Breyton et al. 2013b; Sverzhinsky et al. 2014) as well as new systems to solubilize membrane proteins (Maric et al. 2014; Midtgaard et al. 2014). Finally, newly developed or upgraded SANS instruments at various neutron sources (Dewhurst et al. 2016; Abbas et al. 2015; Jaksch et al. 2014; Heller et al. 2014; Liu et al. 2013) will improve the accessibility and impact of the technique further and open it to a broader scientific community.

Appendix

This appendix provides detailed equations of amplitudes (i.e. weighted form factors) of the geometrical shapes presented in Figs. 12.1 and 12.3. They are modified after a book chapter by Pedersen (Pedersen 2002).

Form factor of a sphere with radius R and volume V:

$$F(q,R) = 3\frac{\sin(qR) - qR\cos(qR)}{(qR)^3}, V(R) = \frac{4}{3}\pi R^3$$

Scattering mass M of a particle with volume V:

$$M = \int_V \Delta\rho dV$$

Amplitude of a micelle with radius R:

$$A_{micelle}(q) = \frac{1}{M_{micelle}}[\Delta\rho_{shell}V_{shell+core}F(q,R) + (\Delta\rho_{core} - \Delta\rho_{shell})V_{core}F(q,R_{core})]$$
$$M_{micelle} = \Delta\rho_{shell}V(R) + (\Delta\rho_{core} - \Delta\rho_{shell})V(R_{core})$$

Amplitude of a protein-detergent complex with radius R:

$$A_{complex}(q) = \frac{1}{M_{complex}}\begin{bmatrix}\Delta\rho_{head}V(R)F(R) + (\Delta\rho_{tail} - \Delta\rho_{head})V(R - R_{head})F(R - R_{head}) \\ +(\Delta\rho_{prot} - \Delta\rho_{tail})V(R - R_{head} - R_{tail})F(R - R_{head} - R_{tail})\end{bmatrix}$$
$$M_{complex} = \Delta\rho_{head}V(R) + (\Delta\rho_{tail} - \Delta\rho_{head})V(R - R_{head}) + (\Delta\rho_{prot} - \Delta\rho_{tail})V(R - R_{head} - R_{tail})$$

References

Abbas S et al (2015) On the design and experimental realization of a multislit-based very small angle neutron scattering instrument at the European spallation source. J Appl Crystallogr 48(4):1242–1253

Ashkar R et al (2015) Tuning membrane thickness fluctuations in model lipid bilayers. Biophys J 109 (1):106–112

Atkinson D, Small DM (1986) Recombinant lipoproteins: implications for structure and assembly of native lipoproteins. Annu Rev Biophys Biophys Chem 15:403–456

Bayburt TH, Sligar SG (2010) Membrane protein assembly into Nanodiscs. FEBS Lett 584(9):1721–1727

Berthaud A, Manzi J, Perez J, Mangenot S (2012) Modeling detergent organization around aquaporin-0 using small-angle x-ray scattering. J Am Chem Soc 134(24):10080–10088

Bouwstra JA, Gooris GS, Bras W, Talsma H (1993) Small angle X-ray scattering: possibilities and limitations in characterization of vesicles. Chem Phys Lipids 64 (1–3):83–98

Breyton C et al (2009) Micellar and biochemical properties of (hemi)fluorinated surfactants are controlled by the size of the polar head. Biophys J 97 (4):1077–1086

Breyton C et al (2013a) Small angle neutron scattering for the study of solubilised membrane proteins. Eur Phys J E Soft Matter 36(7):71

Breyton C et al (2013b) Assessing the conformational changes of pb5, the receptor-binding protein of phage T5, upon binding to its Escherichia coli receptor FhuA. J Biol Chem 288(42):30763–30772

Bu Z, Engelman DM (1999) A method for determining transmembrane helix association and orientation in detergent micelles using small angle x-ray scattering. Biophys J 77(2):1064–1073

Bu Z, Wang L, Kendall DA (2003) Nucleotide binding induces changes in the oligomeric state and conformation of Sec A in a lipid environment: a small-angle neutron-scattering study. J Mol Biol 332(1):23–30

Calcutta A et al (2012) Mapping of unfolding states of integral helical membrane proteins by GPS-NMR and scattering techniques: TFE-induced unfolding of KcsA in DDM surfactant. Biochim Biophys Acta 1818(9):2290–2301

Cardoso MB, Smolensky D, Heller WT, O'Neill H (2009) Insight into the structure of light-harvesting complex II and its stabilization in detergent solution. J Phys Chem B 113(51):16377–16383

Chacon P, Moran F, Diaz JF, Pantos E, Andreu JM (1998) Low-resolution structures of proteins in solution retrieved from X-ray scattering with a genetic algorithm. Biophys J 74(6):2760–2775

Charles M, Semeriva M, Chabre M (1980) Small-angle neutron scattering study of the association between porcine pancreatic colipase and taurodeoxycholate micelles. J Mol Biol 139(3):297–317

Chaudhuri BN (2015) Emerging applications of small angle solution scattering in structural biology. Protein Sci 24(3):267–276

Chen PC, Hub JS (2015) Structural properties of protein-detergent complexes from SAXS and MD simulations. J Phys Chem Lett 6(24):5116–5121

Clifton LA et al (2012) Low resolution structure and dynamics of a colicin-receptor complex determined by neutron scattering. J Biol Chem 287(1):337–346

Clifton LA, Neylon C, Lakey JH (2013) Examining protein-lipid complexes using neutron scattering. Methods Mol Biol 974:119–150

Columbus L et al (2006) Expression, purification, and characterization of Thermotoga maritima membrane proteins for structure determination. Protein Sci 15 (5):961–975

Compton EL, Karinou E, Naismith JH, Gabel F, Javelle A (2011) Low resolution structure of a bacterial SLC26 transporter reveals dimeric stoichiometry and mobile intracellular domains. J Biol Chem 286 (30):27058–27067

Compton EL et al (2014) Conserved structure and domain organization among bacterial Slc26 transporters. Biochem J 463(2):297–307

D'Andrea MG et al (2011) Thermodynamic and structural characterization of zwitterionic micelles of the membrane protein solubilizing amidosulfobetaine surfactants ASB-14 and ASB-16. Langmuir 27 (13):8248–8256

Dewhurst CD et al (2016) The small-angle neutron scattering instrument D33 at the Institut Laue-Langevin. J Appl Crystallogr 49(1):1–14

Dovling Kaspersen J et al (2014) Low-resolution structures of OmpADDM protein-detergent complexes. Chembiochem 15(14):2113–2124

Efremov RG, Leitner A, Aebersold R, Raunser S (2015) Architecture and conformational switch mechanism of the ryanodine receptor. Nature 517(7532):39–43

Gabel F et al (2002) Protein dynamics studied by neutron scattering. Q Rev Biophys 35(4):327–367

Gabel F et al (2014) Probing the conformation of FhaC with small-angle neutron scattering and molecular modeling. Biophys J 107(1):185–196

Gobl C et al (2010) Influence of phosphocholine alkyl chain length on peptide-micelle interactions and micellar size and shape. J Phys Chem B 114 (13):4717–4724

Gohon Y et al (2008) Bacteriorhodopsin/amphipol complexes: structural and functional properties. Biophys J 94(9):3523–3537

Haas H et al (2004) Small angle x-ray scattering from lipid-bound myelin basic protein in solution. Biophys J 86(1 Pt 1):455–460

Haertlein M et al (2016) Biomolecular Deuteration for neutron structural biology and dynamics. Methods Enzymol 566:113–157

Harroun TA et al (2005) Comprehensive examination of mesophases formed by DMPC and DHPC mixtures. Langmuir 21(12):5356–5361

Helenius A, Simons K (1975) Solubilization of membranes by detergents. Biochim Biophys Acta 415(1):29–79

Heller WT et al (2014) The bio-SANS instrument at the high flux isotope reactor of Oak Ridge National Laboratory. J Appl Crystallogr 47(4):1238–1246

Herrera FE, Garay AS, Rodrigues DE (2014) Structural properties of CHAPS micelles, studied by molecular dynamics simulations. J Phys Chem B 118 (14):3912–3921

Hiruma-Shimizu K, Shimizu H, Thompson GS, Kalverda AP, Patching SG (2016) Deuterated detergents for structural and functional studies of membrane proteins: properties, chemical synthesis and applications. Mol Membr Biol 32:1–17

Hong X, Weng YX, Li M (2004) Determination of the topological shape of integral membrane protein light-harvesting complex LH2 from photosynthetic bacteria in the detergent solution by small-angle X-ray scattering. Biophys J 86(2):1082–1088

Hunt JF, McCrea PD, Zaccai G, Engelman DM (1997) Assessment of the aggregation state of integral membrane proteins in reconstituted phospholipid vesicles using small angle neutron scattering. J Mol Biol 273 (5):1004–1019

Jacques DA, Trewhella J (2010) Small-angle scattering for structural biology – expanding the frontier while avoiding the pitfalls. Protein Sci 19(4):642–657

Jacrot B (1976) The study of biological structures by neutron scattering from solution. Rep Prog Phys 39 (10):911–953

Jaksch S et al (2014) Concept for a time-of-flight small angle neutron scattering instrument at the European spallation source. Nucl Instrum Methods Phys Res, Sect A 762:22–30

Johs A et al (2006) Modular structure of solubilized human apolipoprotein B-100. Low resolution model revealed by small angle neutron scattering. J Biol Chem 281(28):19732–19739

Jordan A et al (2016) SEC-SANS: size exclusion chromatography combined in situ with small-angle neutron scattering. J Appl Crystallogr 49(6):2015–2020

Joseph JS et al (2011) Characterization of lipid matrices for membrane protein crystallization by high-throughput small angle X-ray scattering. Methods 55 (4):342–349

Khvostichenko DS et al (2013) An x-ray transparent microfluidic platform for screening of the phase behavior of lipidic mesophases. Analyst 138 (18):5384–5395

Kondrashkina E et al (2013) Using macromolecular-crystallography beamline and microfluidic platform for small-angle diffraction studies of lipidic matrices for membrane-protein crystallization. J Phys Conf Ser 425:012013

Koutsioubas A, Berthaud A, Mangenot S, Perez J (2013) Ab initio and all-atom modeling of detergent organization around Aquaporin-0 based on SAXS data. J Phys Chem B 117(43):13588–13594

Kynde SA et al (2014) Small-angle scattering gives direct structural information about a membrane protein inside a lipid environment. Acta Crystallogr D Biol Crystallogr 70(Pt 2):371–383

Le RK et al (2014) Analysis of the solution structure of Thermosynechococcus elongatus photosystem I in n-dodecyl-beta-D-maltoside using small-angle neutron scattering and molecular dynamics simulation. Arch Biochem Biophys 550–551:50–57

Le Roy A et al (2015) AUC and small-angle scattering for membrane proteins. Methods Enzymol 562:257–286

Lipfert J, Columbus L, Chu VB, Lesley SA, Doniach S (2007) Size and shape of detergent micelles determined by small-angle X-ray scattering. J Phys Chem B 111(43):12427–12438

Liu D et al (2013) Demonstration of a novel focusing small-angle neutron scattering instrument equipped with axisymmetric mirrors. Nat Commun 4:2556

le Maire M, Champeil P, Moller JV (2000) Interaction of membrane proteins and lipids with solubilizing detergents. Biochim Biophys Acta 1508(1–2):86–111

Manet S et al (2011) Structure of micelles of a nonionic block copolymer determined by SANS and SAXS. J Phys Chem B 115(39):11318–11329

Maric S et al (2014) Stealth carriers for low-resolution structure determination of membrane proteins in solution. Acta Crystallogr D Biol Crystallogr 70 (Pt 2):317–328

Maric S et al (2015) Biosynthetic preparation of selectively deuterated phosphatidylcholine in genetically modified Escherichia coli. Appl Microbiol Biotechnol 99(1):241–254

Midtgaard SR et al (2014) Self-assembling peptides form nanodiscs that stabilize membrane proteins. Soft Matter 10(5):738–752

Nakano M et al (2009) Static and dynamic properties of phospholipid bilayer nanodiscs. J Am Chem Soc 131 (23):8308–8312

Nogales A et al (2010) Three-dimensional model of human platelet integrin alphaIIb beta3 in solution obtained by small angle neutron scattering. J Biol Chem 285(2):1023–1031

Oliver RC et al (2013) Dependence of micelle size and shape on detergent alkyl chain length and head group. PLoS One 8(5):e62488

O'Malley MA, Helgeson ME, Wagner NJ, Robinson AS (2011) Toward rational design of protein detergent complexes: determinants of mixed micelles that are critical for the in vitro stabilization of a G-protein coupled receptor. Biophys J 101(8):1938–1948

O'Neill H, Heller WT, Helton KE, Urban VS, Greenbaum E (2007) Small-angle X-ray scattering study of photosystem I-detergent complexes: implications for membrane protein crystallization. J Phys Chem B 111 (16):4211–4219

Osborne HB, Sardet C, Michel-Villaz M, Chabre M (1978) Structural study of rhodopsin in detergent micelles by small-angle neutron scattering. J Mol Biol 123(2):177–206

Pedersen JS (2002) Modelling of small-angle scattering data from colloids and polymer systems. In: Lindner P, Zemb T (eds) Neutrons, x-rays and light: scattering methods applied to soft condensed matter. Elsevier, Amsterdam, pp 391–420

Perez J, Koutsioubas A (2015) Memprot: a program to model the detergent corona around a membrane protein based on SEC-SAXS data. Acta Crystallogr D Biol Crystallogr 71(Pt 1):86–93

Perkins SJ, Weiss H (1983) Low-resolution structural studies of mitochondrial ubiquinol: cytochrome c reductase in detergent solutions by neutron scattering. J Mol Biol 168(4):847–866

Perlmutter JD et al (2011) All-atom and coarse-grained molecular dynamics simulations of a membrane protein stabilizing polymer. Langmuir 27 (17):10523–10537

Petoukhov MV, Svergun DI (2006) Joint use of small-angle X-ray and neutron scattering to study biological macromolecules in solution. Eur Biophys J 35 (7):567–576

Petoukhov MV et al (2012) New developments in the program package for small-angle scattering data analysis. J Appl Crystallogr 45(Pt 2):342–350

Qian S, Heller WT (2011) Peptide-induced asymmetric distribution of charged lipids in a vesicle bilayer revealed by small-angle neutron scattering. J Phys Chem B 115(32):9831–9837

Qian S, Heller WT (2015) Melittin-induced cholesterol reorganization in lipid bilayer membranes. Biochim Biophys Acta 1848(10 Pt A):2253–2260

Rubinson KA, Pokalsky C, Krueger S, Prochaska LJ (2013) Structure determination of functional membrane proteins using small-angle neutron scattering (sans) with small, mixed-lipid liposomes: native beef heart mitochondrial cytochrome c oxidase forms dimers. Protein J 32(1):27–38

Seddon AM, Curnow P, Booth PJ (2004) Membrane proteins, lipids and detergents: not just a soap opera. Biochim Biophys Acta 1666(1–2):105–117

Sharma KS et al (2012) Non-ionic amphiphilic homopolymers: synthesis, solution properties, and biochemical validation. Langmuir 28(10):4625–4639

Skar-Gislinge N, Arleth L (2011) Small-angle scattering from phospholipid nanodiscs: derivation and refinement of a molecular constrained analytical model form factor. Phys Chem Chem Phys 13 (8):3161–3170

Skar-Gislinge N et al (2010) Elliptical structure of phospholipid bilayer nanodiscs encapsulated by scaffold proteins: casting the roles of the lipids and the protein. J Am Chem Soc 132(39):13713–13722

Stuhrmann HB (1973) Comparison of the three basic scattering functions of myoglobin in solution with those from the known structure in crystalline state. J Mol Biol 77(3):363–369

Stuhrmann HB et al (1975) Neutron scattering study of human serum low density lipoprotein. Proc Natl Acad Sci U S A 72(6):2270–2273

Svergun DI (1999) Restoring low resolution structure of biological macromolecules from solution scattering using simulated annealing. Biophys J 76 (6):2879–2886

Svergun DI et al (1998) Protein hydration in solution: experimental observation by x-ray and neutron scattering. Proc Natl Acad Sci U S A 95(5):2267–2272

Sverzhinsky A et al (2014) Amphipol-trapped ExbB-ExbD membrane protein complex from Escherichia coli: a biochemical and structural case study. J Membr Biol 247(9–10):1005–1018

Tang KH, Urban VS, Wen J, Xin Y, Blankenship RE (2010) SANS investigation of the photosynthetic machinery of Chloroflexus aurantiacus. Biophys J 99 (8):2398–2407

Timmins PA, Zaccai G (1988) Low resolution structures of biological complexes studied by neutron scattering. Eur Biophys J 15(5):257–268

Watanabe Y, Inoko Y (2005) Physicochemical characterization of the reassembled dimer of an integral membrane protein OmpF porin. Protein J 24(3):167–174

Wise DS, Karlin A, Schoenborn BP (1979) An analysis by low-angle neutron scattering of the structure of the acetylcholine receptor from Torpedo californica in detergent solution. Biophys J 28(3):473–496

Wright GS, Hasnain SS, Grossmann JG (2011) The structural plasticity of the human copper chaperone for SOD1: insights from combined size-exclusion chromatographic and solution x-ray scattering studies. Biochem J 439(1):39–44

Yeager MJ (1976) Neutron diffraction analysis of the structure of retinal photoreceptor membranes and rhodopsin. Brookhaven Symp Biol 27:III3–III36

Zaccai NR et al (2016) Deuterium labeling together with contrast variation small-angle neutron scattering suggests how Skp captures and releases unfolded outer membrane proteins. Methods Enzymol 566:159–210

Zimmer J, Doyle DA, Grossmann JG (2006) Structural characterization and pH-induced conformational transition of full-length KcsA. Biophys J 90 (5):1752–1766